https://doi.org/10.1038/s44459-026-00056-9

Indoor neutral-host networks over shared spectrum and shared infrastructure: a comparison study of real-world deployments

Check for updates

Joshua Roy Palathinkal[1] ✉, Muhammad Iqbal Rochman[1], Vanlin Sathya[2], Mehmet Yavuz[2] & Monisha Ghosh[1]

Indoor high-capacity connectivity is often constrained by significant building penetration loss and uplink power limitations of outdoor macro-cells. While Mobile Network Operators (MNOs) optimize low-band (<1 GHz) and mid-band (1–7 GHz) spectrum, uplink performance remains disproportionately degraded due to link budget asymmetry. Neutral-host (NH) networking offers a scalable alternative by transparently offloading MNO subscribers via spectrum sharing and shared infrastructure. We present a multi-site study comparing CBRS–enabled NH networks, public MNO 4G/5G, and Wi-Fi. Our results show: (i) significant building penetration loss (up to 17.9 dB in mid-bands) creates a ~10 dB RSRP deficit for MNO mid-bands versus low-bands; (ii) NH networks provide 30 dB higher median indoor RSRP, with indoor NH normalized downlink throughput matching MNO outdoor performance and NH uplink exceeding MNO levels in all settings; (iii) NH proximity enables superior efficiency, utilizing 64-QAM for 56% of transmissions (versus <6% for MNOs) and reducing median UE transmit power by 5 dB; (iv) MNOs rely on low-bands for indoor uplink, whereas NH maintains high-performance mid-band connectivity; and (v) NH outperforms MNOs in end-to-end throughput but trails Wi-Fi in uplink throughput and latency due to core routing overhead.

Mobile network consumers expect indoor cellular performance to mirror the reliability of outdoor connectivity. Despite South Korea leading the world with 100% 5G coverage and the highest density of 5G radio base station (gNB) (670 gNBs per 100,000 inhabitants)[1], user satisfaction for 5G remains lower than that of 4G, primarily due to inadequate indoor performance[2] leading to a focus on improving indoor connectivity[3]. In the U.S., mid-band spectrum (1–7 GHz) has become the preferred choice over low-band (<1 GHz) for delivering high-performance 5G, owing to its superior bandwidth availability. For instance, public Mobile Network Operators (MNOs) have utilized the 3.45–3.55 GHz and 3.7–3.98 GHz bands for commercial 5G deployments. However, consistent indoor connectivity is hindered by significant building penetration loss. Modern energy-efficient construction, particularly the use of low-emissivity (Low-E) glass, exacerbates this by substantially increasing RF attenuation at the mid-band frequencies critical for 5G.

Further, the performance of the uplink is disproportionately degraded relative to an already attenuated downlink. This occurs because a gNB transmits at power levels hundreds of times higher than the maximum user equipment (UE) transmit power, making uplink the limiting link budget component. MNOs have attempted to mitigate these issues by deploying low-band (<1 GHz) to exploit better propagation characteristics and increase gNB site density[4]. However, these approaches merely alleviate symptoms rather than resolve the fundamental imbalance in indoor propagation and uplink constraints. Furthermore, operators may opt for solutions such as Distributed Antenna Systems (DAS) to improve indoor coverage. A DAS distributes cellular signals indoors but relies on an intricate network of passive cabling and specialized RF antennas, and is thus often cost-prohibitive, labor-intensive, and difficult to scale.

The high cost and complexity of maintaining DAS deployments have driven the adoption of neutral-host (NH) models, which allow MNOs to offload infrastructure risks to third parties. There is a diverse range of commercially available NH architecture, offering varying trade-offs between cost efficiency, operational control, and deployment complexity. At the foundational level, "passive sharing" allows operators to share

[1]University of Notre Dame, Notre Dame, IN, USA. [2]Celona Inc., Campbell, CA, USA. ✉e-mail: joshuaroy873@gmail.com

non-electronic physical elements such as sites, masts, indoor cabling, and antennas. At a deeper network integration, Multi-Operator Radio Access Network (MORAN) enables MNOs to share base stations and radio equipment while retaining their own dedicated spectrum and core networks. Alternatively, Multi-Operator Core Network (MOCN) sharing extends this integration by allowing MNOs to share both the RAN infrastructure and the radio spectrum, though traffic is still routed to each operator's distinct core network. Finally, the use of private cellular networks allows enterprises or third parties to deploy localized, dedicated infrastructure.

Although these diverse NH approaches effectively reduce capital and operational expenditures, traditional active sharing models still require the complex coordination of exclusive MNO-licensed spectrum. To address this, our paper focuses on a shared-spectrum NH model utilizing MOCN architecture. This approach enables sharing of a dedicated private cellular network by MNO subscribers using the shared-licensed spectrum, specifically, the 3.55 GHz Citizens Broadband Radio Service (CBRS) band in the US[5]. This approach enables private 4G/5G networks that can provide seamless indoor connectivity for public MNO subscribers. For the remainder of this work, the acronym "NH" designates the shared-spectrum neutral-host architecture.

Figure 1 illustrates the architecture of the shared-spectrum neutral-host network discussed in this work. The left side of the diagram depicts the deployment at the customer premises, consisting of UEs connected to CBSDs, alongside edge private cores that manage the radio devices. The center of the figure highlights the MOCN gateway, which facilitates neutral-host sharing by routing MNO subscriber traffic from the CBSDs to their respective MNO core networks, shown on the right. Upon detecting an NH band, the UE retrieves a list of Public Land Mobile Network (PLMN) IDs from the broadcast network signature. This list represents a white list of MNOs with active commercial agreements with the NH operator. If the subscriber's MNO is present, the device performs a handover to the neutral-host network without requiring user actions or authentication. Once connected to the CBRS base station (i.e., CBSD/CBRS device), the subscriber's data packets are routed to the respective MNO core via an MOCN gateway[6], while also being secured by IPsec tunnels. This architecture establishes a secure tunnel, allowing the user to access data services authenticated by the SIM credentials associated with their existing service plan. Note that this gateway-based approach is slightly different from the traditional MOCN, where MNO cores are directly integrated into the shared RAN through a direct, carrier-grade connection (e.g., leased fiber, Carrier Ethernet).

The adoption of NH architecture offers a viable path to mitigate building penetration loss and uplink power constraints. This study contributes an empirical analysis of on-site measurements of co-located NH, 4G/5G MNO and 2.4/5 GHz Wi-Fi deployments at three distinct sites. This comparative data provides a foundational framework for future mid-band spectrum sharing studies, particularly for the 3.1–3.45 GHz and 7.125–8.4 GHz bands currently being studied by the National Telecommunications and Information Administration (NTIA) for shared use[7]. Recent U.S. spectrum policy developments further underscore the strategic importance of these bands. The December 2025 Presidential Memorandum on *"Winning the 6G Race"* directs federal agencies to initiate studies toward reallocation of portions of the 7.125–7.4 GHz band for commercial licensed use, including evaluation of relocation into adjacent spectrum such as 7.4–8.4 GHz[8]. The memorandum also calls for feasibility studies of the 2.69–2.9 GHz and 4.4–4.94 GHz bands for potential reallocation. Further, in January 2026, the Federal Communications Commission (FCC) in the U.S. started a Notice of Proposed Rulemaking (NPRM) to explore reallocation of the Upper C-band, 3.98–4.2 GHz[9]. Since radar altimeters operating in the adjacent 4.2–4.4 GHz band will need to be protected, it is unlikely that high-power exclusive licensing will be feasible in the entire band. The lessons learned from shared-spectrum usage in the CBRS band can inform spectrum sharing in part of the Upper C-band[10,11]. These initiatives highlight the increasing emphasis on mid- and upper-mid-band spectrum as foundational resources for future 6G systems and motivate empirical evaluation of indoor deployment and spectrum reuse models.

While indoor NH networks can be deployed on any spectrum, overall spectrum utilization is maximized by reusing spectrum that has primarily outdoor incumbents, like in the CBRS band: incumbents can continue operation without interference while the spectrum can be shared by low-power indoor networks. Thus, the building loss, instead of being a liability, becomes an enabler of sharing spectrum.

Our contributions are as follows:

- *Comparison of building loss between three sites with distinct signal environments*: MNO macro deployments across all sites exhibit significant building penetration loss, reaching 15.5 dB in low-bands and 17.9 dB in mid-bands. Furthermore, median mid-band RSRP is consistently lower than low-band (~10.8 dB indoors and ~10 dB outdoors). These results underscore the critical role of low-band spectrum in ensuring indoor coverage, even where mid-bands offer superior peak capacity.
- *Comparison of coverage and physical layer performance*: The NH network exhibits significantly higher indoor signal strength, with a median RSRP of −89.9 dBm compared to −120.2 dBm for MNO macro deployments. While indoor MNO coverage is improved by a dedicated outdoor small-cell deployment, the neutral-host still provides a comparable normalized downlink physical-layer (PHY) throughput. In the uplink PHY-layer, the indoor NH solution outperforms MNO performance in both indoor and outdoor environments.
- *Focused analysis of uplink metrics* : Uplink performance data confirms a clear NH advantage in indoors, with 64-QAM utilized for 56% of transmissions compared to less than 6% for MNO macro networks. Correspondingly, the NH sustains substantially higher uplink and

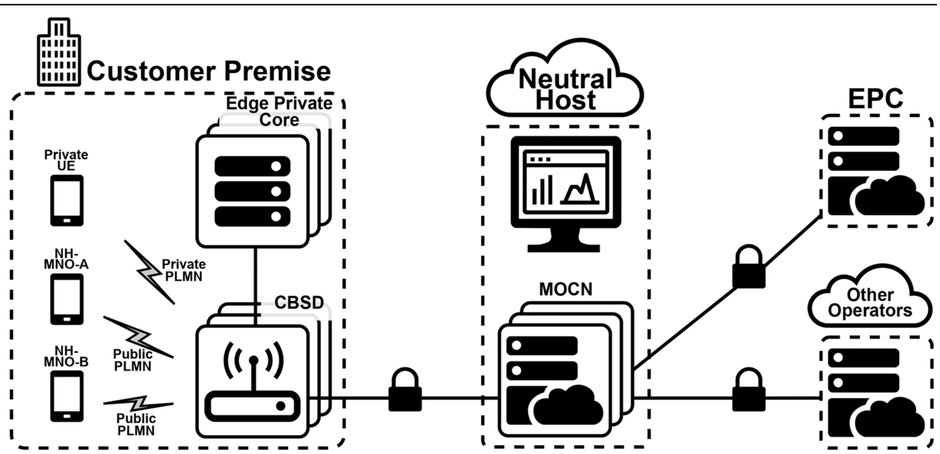

Fig. 1 | Neutral-host architecture (reproduced from ref. 17, with permission from IEEE).

downlink PHY-layer MCS indices, reflecting more efficient link adaptation. This efficiency is coupled with a 5 dB reduction in median UE TX power, driven by the shorter propagation paths of the NH deployment. The data also reveals a distinct shift in 5G band utilization by the MNOs—while mid-bands dominate outdoor traffic, their usage drops significantly indoors, highlighting that low-band spectrum remains the primary anchor for indoor uplink reliability.

- *Comparison of end-to-end network performance*: Our analysis reveals a performance trade-off where NH exceeds MNO indoor throughput but trails Wi-Fi in UL throughput and latency. We show that Wi-Fi median UL throughput is 1.8× higher than NH at matched 20 MHz bandwidth, an advantage that scales to 10.7× when Wi-Fi utilizes double the bandwidth of the NH network. This underscores the critical necessity for protocol and routing optimizations to achieve uplink and latency performance parity.

Related works

There is a lack of extensive literature on NH network deployments, specifically regarding real-world coverage, coexistence, and performance. For instance, [12,13] provide analyses of spectrum capacity and reuse based on deployment simulations. Other work [5,14–16] provides high-level performance analysis based on real-world deployment, but lacks detailed analyses of PHY signal coverage and resource utilization. On the other hand, our prior works[17,18] provide a detailed breakdown of NH performance to generalize the benefits of NH infrastructure over the traditional MNO macro networks. These analyses are conducted based on measurements from different environments:[17] focuses on a hospital setting, while[18] analyzes a big-box retail location. In both cases, the NH network operates on the CBRS band, which utilizes a spectrum-sharing model to coexist with outdoor incumbents, such as naval radar[19]. This framework creates a unique opportunity for low-power indoor private 4G/5G networks to operate without interfering with incumbents. Simultaneously, it provides robust indoor coverage that traditional outdoor MNO macro deployments struggle to achieve, while offering a vital avenue to offload heavy indoor traffic from the macro network. In this paper, we seek to extend the prior research by focusing specifically on uplink performance: it is becoming increasingly clear that many advanced 5G and future 6G applications will require improved uplink performance, and many of these will be deployed indoors, such as factory and warehouse automation.

Methods

Measurement methodology

We utilized a Samsung S22+ smartphone capable of connecting to all relevant bands—4G/5G cellular, Wi-Fi and CBRS neutral-host bands. QualiPoc and SigCap measurement tools were employed to obtain wireless Key Performance Indicator (KPI) metrics for comparative network evaluations. Passive KPIs (*e.g.*, signal strength metrics such as RSRP for LTE, SS-RSRP for NR, and RSSI for Wi-Fi) were continuously recorded by QualiPoc and SigCap, respectively. For active probe measurements, the QualiPoc tool executed a predefined test sequence comprising: (i) a 5-s HTTP download from *github.com* utilizing the HTTP GET command; (ii) a 5-s HTTP upload to *httpbin.org* utilizing the HTTP PUT command; and (iii) ten ICMP echo requests (32-byte packets) to the *Google DNS (8.8.8.8)* host. QualiPoc collects detailed LTE and NR PHY-layer measurements by directly probing the modem chipset through the *Qualcomm Diagnostic Mode* interface[20]. In contrast, SigCap is limited to the information exposed by the Android API and was therefore used exclusively for Wi-Fi analysis[21]. Table 1 summarizes the QualiPoc and SigCap KPIs employed in this study.

In this study, we measured data from two deployment locations: *a big-box retail store* and *a refinery complex*. Within the refinery complex, we further focus on two separate buildings, thus totaling three sites. Figure 2 illustrates the three sites which represent distinct signal environments:

- *Site*-A is a big-box retail store in the suburban area. This site is characterized by thick concrete walls and minimal windows.
- *Site-B* is an office building within the refinery complex, characterized by large low-emission (low-e) glass windows and dry walls.
- *Site-C* is a warehouse annex in the refinery complex. It is characterized by metal structures and walls, as well as industrial equipment.In all sites, both indoor CBSD and Wi-Fi access points (APs) are deployed facing down on the ceiling.

The measurements were conducted by walking indoors and outdoors, in three separate campaigns between September and December of 2025, collecting a total of over 10 h of data. Three major cellular MNOs (labeled MNO-A, MNO-B, and MNO-C) are available in all three sites, with only MNO-A & B having commercial agreements to offload their subscribers to the neutral-host. In total, there are 254,728 datapoints captured over the QualiPoc radio reports, PDSCH (downlink) throughput, PUSCH (uplink) throughput, and application-layer (HTTP session and ping logs) reports, as well as 126,790 Wi-Fi beacon datapoints captured by SigCap. Network-side traffic load information is proprietary to the MNOs and not available in this UE-centric study. All measurements were therefore conducted during typical working hours to reflect performance under realistic, live-network conditions.

Deployment: overview

Figure 3 illustrates the cellular measurement footprints for Sites A, B, and C, aggregating measurements across all deployments (macro and neutral-host), operators (MNO-A, B, C), and radio access technologies (LTE, NR). The maps depict the average signal strength, computed using RSRP for LTE and SS-RSRP for NR, and spatially averaged over 7.5 × 7.5 m square bins.

While Site-A provided comprehensive indoor and outdoor coverage, Sites B and C exhibited spatial constraints. Site-B's outdoor measurements were restricted to the building's immediate perimeter, while Site-C were restricted to the immediate west of the building. Further, Site-B's indoor data suffered from significant GPS attrition: approximately 69,000 data points across varying timestamps reported identical coordinates. This indicates a GPS failure that limited the usable indoor measurement region. Despite this lack of spatial data, these data points are retained in our analysis as the study focuses on performance metrics rather than spatial correlations.

Table 2 highlights the distinct physical layer configuration across operators. For all operators, 4G bands (denoted with the prefix '*b*') typically use FDD, except for the TDD-based b48 (i.e., the CBRS band). Most 5G mid-bands utilized TDD and 30 kHz SCS, though n25 followed the low-band convention of FDD and 15 kHz SCS. Channel bandwidths for 4G and 5G low bands typically ranged between 5 and 20 MHz, whereas 5G mid bands (e.g., n41 and n77) reached up to 100 MHz. While 5G Non-Standalone (NSA) mode was the standard across all MNOs, MNO-B additionally utilized Standalone (SA) mode. Notably, the CBRS band (designated as band b48 per 3GPP standards) was not only utilized by the private NH network, but also by MNO-C in a macro-cell configuration.

Deployment: MNO macro

Site-specific variations in band configurations for both indoor (IN) and outdoor (OUT) environments are summarized in Table 3. Based on the count of unique Physical Cell Identifiers (PCIs), we observe a significantly lower NR deployment density compared to LTE. Notably, mid-band frequencies (indicated in **bold**) exhibit reduced indoor availability, with fewer unique PCIs detected indoors than outdoors. Regarding network architecture, although MNO-B utilizes both 5G SA and NSA modes, SA mode was observed exclusively in outdoor measurements. Furthermore, MNO-C's CBRS (b48) deployments were primarily restricted to outdoor regions. These observations are consistent with the expected effects of building penetration loss on mid-band and high-frequency signal propagation.

Deployment: CBRS neutral-host

The neutral-host infrastructure at all three sites utilizes identical indoor CBSD models provided by Celona, Inc., operating in the 4G LTE within the 3GPP Release-13 standard. Each unit is configured with two PCIs at a 20 MHz channel bandwidth, enabling intra-CBSD carrier aggregation (CA)

Table 1 | Summary of captured network performance parameters

Parameter	Description
Qualipoc & SigCap: General parameters	
Latitude, Longitude	UE's geographic coordinates
Qualipoc: Radio report parameters	
PCI	Physical cell identifier
DL/UL ARFCN	Absolute radio frequency channel number, i.e., center frequency
Bandwidth	Range of frequencies available for transmission [MHz]
RSRP	Reference signal received power. For NR, RSRP is based on the synchronization signal (SS) block [dBm]
Qualipoc: Performance & power metrics	
Normalized PDSCH/PUSCH throughput	PHY-layer throughput on the physical downlink/uplink shared channel, normalized by allocated resource blocks, subcarrier spacing, and MIMO layers [bit/s/Hz/stream][22]
PDSCH/PUSCH modulation	Modulation scheme used on the physical shared channel, e.g., QPSK, 16-QAM, 64-QAM
PUSCH TX power	UE's PUSCH uplink transmit power [dBm]
HTTP GET/PUT test status	Application-layer test outcome for HTTP downlink (GET) and uplink (PUT) transactions, indicating success or failure of end-to-end data transfer
IP DL/UL throughput	Network-layer throughput in downlink/uplink [Mbps]
Round-trip Time (RTT)	Measured RTT from ICMP ping
SigCap: Wi-Fi parameters	
BSSID	Basic service set identifier (unique identifier of a Wi-Fi AP)
Primary channel number	Primary channel associated with the BSSID [MHz]
RSSI	Received signal strength indicator from the beacon signal [dBm]
TX power	Conducted transmit power of the BSSID [dBm]

Fig. 2 | Overview of deployment sites.

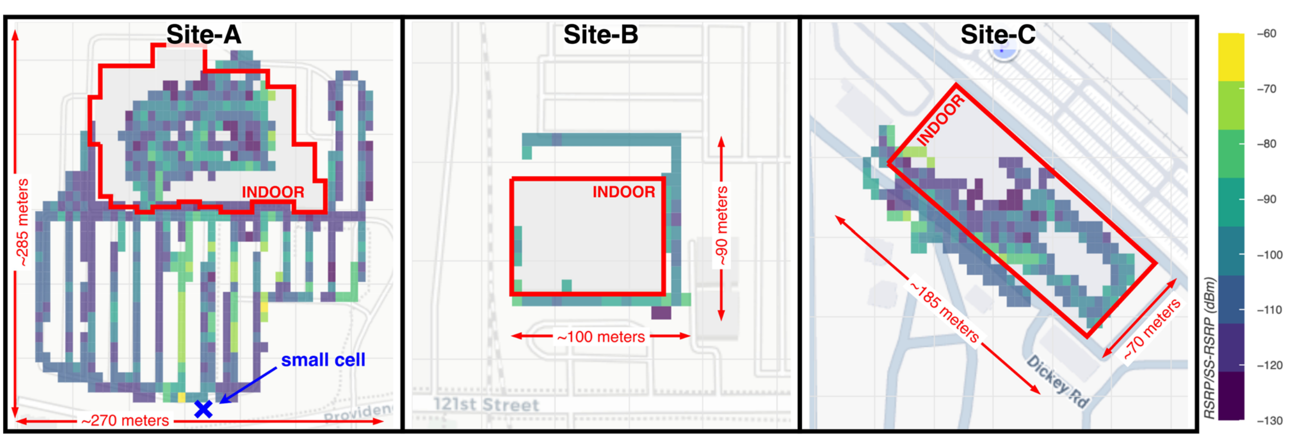

Fig. 3 | Cellular measurement footprint for Sites A, B, and C.

Table 2 | 4G and 5G bands information

Operator	Band	Duplex Mode	DL Band Freq. (MHz)	SCS (kHz)	DL BW (MHz)
			NR bands		
MNO-A	n5	FDD	850	15	10
	n77	TDD	3700	30	40, 80
MNO-B	n25	FDD	1900	15	10, 15, 20, 40
	n41	TDD	2500	30	90, 100
	n71	FDD	600	15	15, 20
MNO-C	n77	TDD	3700	30	60, 100
			LTE bands		
NH	b48	TDD	3500	15	20
MNO-A	b2	FDD	1900	15	5, 10, 20
	b4	FDD	2100	15	20
	b12	FDD	700	15	10
	b14	FDD	700	15	5, 10
	b30	FDD	2300	15	5, 10
	b66	FDD	2100	15	5, 10
MNO-B	b2	FDD	1900	15	5, 10
	b4	FDD	2100	15	10, 20
	b12	FDD	700	15	5, 10
	b66	FDD	2100	15	20
	b71	FDD	600	15	5
MNO-C	b2	FDD	1900	15	15
	b4	FDD	2100	15	20
	b5	FDD	850	15	10
	b13	FDD	700	15	10
	b48	TDD	3500	15	10, 20
	b66	FDD	2100	15	20

Table 3 | MNO macro deployment summary (bands in bold indicate mid-bands)

Operator	IN/OUT	Bands		#PCI	
		LTE	NR	LTE	NR
		Site-A			
MNO-A	IN	**b2**, b12, b14, **b30, b66**	n5	65	1
	OUT	**b2, b4**, b12, b14, **b30, b66**	n5, **n77**	93	5
MNO-B	IN	**b2, b4**, b12, b71	**n25, n41**, n71	67	3
	OUT	**b2, b4**, b12, **b66**	**n25, n41**, n71	39	4
MNO-C	IN	**b2, b4**, b5, b13, **b66**	–	14	–
	OUT	**b2, b4**, b5, b13, **b48, b66**	**n77**	51	1
		Site-B			
MNO-A	IN	**b2, b4**, b12, **b30, b66**	n5, **n77**	16	4
	OUT	**b2, b4**, b12, b14, **b30, b66**	**n77**	43	1
MNO-B	IN	**b2, b4**, b12, **b66**, b71	**n41**, n71	20	4
	OUT	**b2, b66**	**n25, n41**, n71	13	4
MNO-C	IN	**b4**, b13	–	14	–
	OUT	**b5**, b13, **b48, b66**	**n77**	20	3
		Site-C			
MNO-A	IN	**b2, b4**, b12, b14, **b30, b66**	**n77**	43	2
	OUT	**b2**, b12, b14, **b30, b66**	–	58	–
MNO-B	IN	**b2, b4**, b12, b71	**n41**, n71	27	5
	OUT	–	**n25, n41**, n71	–	3
MNO-C	IN	**b4**, b5, b13, **b48, b66**	**n77**	50	1
	OUT	**b4**, b5, b13, **b48, b66**	**n77**	41	3

for a total bandwidth of 40 MHz; notably, inter-CBSD CA is not supported. The CBSDs support up to 2 × 2 MIMO on both downlink and uplink, and up to 64-QAM modulation. Moreover, they feature a maximum possible transmit power of 24 dBm and utilize internal omnidirectional antennas with a 6 dBi gain.

Across all sites, the CBSDs are deployed as small cells and connected to the enterprise wired network via Ethernet (as shown in Fig. 4). An Edge server is also installed at each site to manage the CBSDs (e.g., handling clock synchronization and MOCN configuration). To serve MNO subscribers, each CBSD establishes an IPsec tunnel to the MOCN, which then routes the traffic to the respective MNOs' core networks through dedicated IPsec tunnels (see Fig. 1).

However, actual configurations for each CBSD are subject to Spectrum Access System (SAS) grants. For instance, 3 out of 10 PCIs at Site-A operated at 23 dBm transmit (TX) power with access to the entire CBRS band. In contrast, all PCIs at Sites B and C were granted 24 dBm but limited to the upper portion of the band (3660–3700 MHz). A comprehensive summary of the deployment configuration is provided in Table 4.

Deployment: enterprise Wi-Fi

Table 5 summarizes the enterprise Wi-Fi deployments across the three test sites. While all sites conventionally used the 2.4 and 5 GHz bands with channel widths up to 40 MHz, the deployments vary significantly in terms of TX power and supported standards (e.g., 802.11n, 11ac, and 11ax). The table additionally reports the median RSSI, providing a representative measure of the signal coverage levels experienced during measurements.

Notably, Site-A features the lowest Wi-Fi AP density (identified by the number of Basic Service Set Identifiers/BSSIDs), despite having the largest indoor area (14,000 m^2) compared to Sites B and C (5000 m^2 and 13,000 m^2, respectively). Additionally, Site-C utilizes two distinct deployments from the same provider: the first deployment, identified by the 802.11n support in 2.4 GHz and 802.11ac support in 5 GHz, while the second is identified by 802.11ax support in both 2.4 and 5 GHz. However, the network is heavily dominated by the latter deployments, which account for approximately 99% of the collected data across both bands.

Results

Several performance distributions in this section are presented using violin plots, which combine kernel density estimation with embedded box plots to illustrate distribution shape alongside median and inter-quartile statistics (P25/P50 (median)/P75). This approach provides a concise summary of multiple network deployments and bands within a single figure. For readability, the median value of each distribution is explicitly annotated on the plot.

Coverage and building loss

Figure 5 illustrates the RSRP/SS-RSRP distributions for neutral-host and MNO macro networks across all evaluated operators, bands, and sites. As expected for an indoor-deployed solution, the NH network exhibits significantly higher indoor signal strength, with a median RSRP of −89.9 dBm compared to −120.2 dBm for MNO macros. For MNO macro deployments, the median indoor-to-outdoor signal strength difference—the measured building loss Δ—is relatively small at approximately 6 dB. This low figure is attributed to the aggregation of various low- and mid-band frequencies in the MNO dataset. In contrast, the neutral-host deployment exhibits a substantially larger median indoor-to-outdoor difference of 26 dB—a predictably higher loss due to higher frequency.

To provide detailed analysis between low-, mid-band MNO macro and NH deployment, Table 6 provides the summary of the median, 25th, and

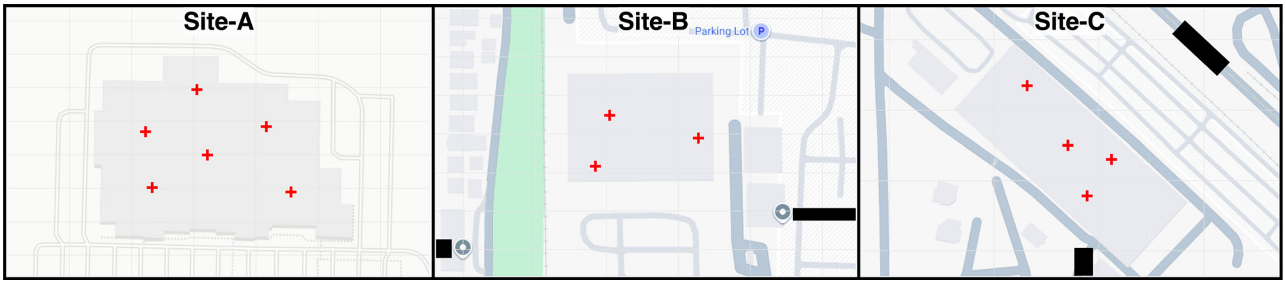

Fig. 4 | CBSD locations at Sites A, B, and C.

Table 4 | Neutral-host deployment parameters across measurement sites

Parameter	Site-A	Site-B	Site-C
#CBSDs/#PCIs	5/10	3/6	4/8
Antenna type	Omnidirectional		
4G TDD config	Config #1: 4 DL & 4 UL subframes		
CBSD transmit power	23, 24 dBm	24 dBm	
Antenna gain	6 dBi		
Center frequency	{3590, 3610, 3630, 3650, 3670, 3690} MHz	{3670, 3690} MHz	
Configured bandwidth	20 MHz		
Channel aggregation	2 channels in downlink (40 MHz), intra-CBSD		

75th percentile values (P25/P75) of SS-RSRP/RSRP, as well as the measured building loss Δ for each site. For the MNO macro, we observe higher Δ at mid-band frequencies than at low-band for Sites A and B, as expected from the increased attenuation characteristics at higher frequencies. In contrast, this trend is not observed for Site-C, likely due to the limited outdoor measurement footprint at that site (illustrated in Fig. 3), which restricts the ability to capture representative outdoor coverage conditions.

Frequency-dependent propagation characteristics create a measurable RSRP gap between MNO bands. As detailed in Table 6, the median RSRP for MNO mid-band is approximately 10.8 dB lower than low-band in indoor environments and 10 dB lower in outdoor settings. From a network management perspective, this implies that a UE undergoing an inter-frequency transition from low- to mid-band will see its RSRP reduced by roughly 10 dB. Such a substantial disparity highlights why low-band spectrum remains critical for indoor coverage, even as MNOs prioritize mid-bands for high-throughput 5G services.

In contrast to these values, the NH deployment exhibits a substantially higher median indoor RSRP compared to the MNO mid-band macro in Table 6, with increases of 43.7 dB, 28.1 dB, and 22.5 dB across Sites A, B, and C, respectively. While these values are inherently site-specific and depend on the density of the surrounding MNO macro deployment, the consistent trend across three distinct sites–together with observations reported in our prior works[17,18]–reinforces the architectural advantage of the NH model. This outcome is a direct consequence of the NH deployment design: as a low-power indoor deployment operating in the b48 mid-band, the signal is optimized for interior coverage and undergoes substantial attenuation when propagating through the building envelope, thereby effectively containing the shared/private coverage footprint within the deployment perimeter.

Looking into Wi-Fi coverage results in Table 5, a similar frequency-dependent trend is observed. Despite denser access point deployments (inferred from #BSSIDs) of 5 GHz compared to 2.4 GHz at Site-A (13 → 54) and Site-B (73 → 171), and comparable at Site-C (118 → 112), the measured median RSSI indicates a consistent degradation when transitioning from 2.4 to 5 GHz operation. Site-B further operates 5 GHz at higher transmit powers (10–11 dBm → 14–16 dBm), while Sites A and C use comparable transmit power levels across bands. Nevertheless, the observed median RSSI reduction when moving from 2.4 to 5 GHz is 11 dB, 8 dB, and 7 dB for Sites A, B, and C, respectively. These results confirm that the propagation advantages of lower frequency bands persist across licensed (MNO), shared (NH) and unlicensed (Wi-Fi) spectrum.

Indoor coverage enhancement via dedicated small cells. To bolster indoor performance at Site-A, MNO-A deployed three outdoor-mounted LTE small-cells operating on bands b2 (PCI-488), b12 (PCI-336), and b66 (PCI-101). These units operate with a 10 MHz channel bandwidth and a 4 × 4 MIMO configuration. The small-cell antennas are oriented northward toward the retail facility, with their specific locations detailed in Fig. 3. While these small cells were deactivated during the aggregate MNO coverage analysis presented in the previous section, they were enabled for this portion of the study to isolate and evaluate their specific impact on the indoor signal environment.

The performance of the small-cell deployment is summarized in Table 6. While the measured building loss Δ remains comparable to macro-only deployments—as the signals still originate from an outdoor source—the localized presence of outdoor small-cells substantially elevates the absolute indoor signal strength. Specifically, the median indoor RSRP improves from −121.4 to −86.9 dBm in low-band operation and from −132.2 to −93.9 dBm in mid-band. Consistent with our earlier findings, the median RSRP of mid-band frequencies is lower than low-band of approximately 7 dB indoors and 6.2 dB outdoors.

PCI-specific analysis. In addition to aggregate signal strength analysis, measurements were also examined on a per-PCI basis to enable a more controlled comparison by focusing on signals from a single base-station source. This approach helps reduce variability associated with mixed cell origins and offers clearer insight into frequency-dependent indoor attenuation.

We first consider NR operation at Site-A, where MNO-B offers measurements spanning both low- and mid-band NR carriers indoors and outdoors. Specifically, PCI-886 (n71, 600 MHz) representing low-band and PCI-764 (n25, 1900 MHz) representing mid-band were selected. The corresponding SS-RSRP distributions are shown in Fig. 6. The median building loss increases from approximately 9 dB at low-band to 15.3 dB at mid-band, indicating substantially higher indoor attenuation at higher frequencies. Although this NR comparison is performed per PCI, the two bands are transmitted from different cells.

To further isolate frequency effects, we analyze LTE deployments where multiple bands are transmitted from the same PCI. This configuration enables a direct comparison of indoor degradation across frequencies originating from an identical source. Two representative cases were selected: PCI-351 at Site-B (MNO-C), operating b13 (700 MHz) and b4 (1700 MHz), and a PCI at Site-C (MNO-B), operating b12 (700 MHz), b66 (1700 MHz), and b30 (2300 MHz). These PCIs provide sufficient indoor measurement density for comparison. As shown in Fig. 7, indoor signal degradation consistently increases with operating frequency, reinforcing the frequency-dependent trends observed in earlier analyses.

Table 5 | Wi-Fi deployment parameters and coverage across measurement sites

Site	Band	#BSSIDs	Bandwidth	TX power	Median RSSI[a]	Standard
Site-A	2.4 GHz	13	20 MHz	14 dBm	−70 dBm	802.11ax
	5 GHz	54	20 MHz	10–16 dBm	−81 dBm	802.11ax
Site-B	2.4 GHz	73	20 MHz	10–11 dBm	−66 dBm	802.11n
	5 GHz	171	40 MHz	14–16 dBm	−74 dBm	802.11ac
Site-C	2.4 GHz	118	20 MHz	3–27 dBm	−69 dBm	802.11n/ax
	5 GHz	112	40 MHz	6–26 dBm	−76 dBm	802.11ac/ax

[a]RSSI measurements reported here were extracted from both beacon signals and active connections.

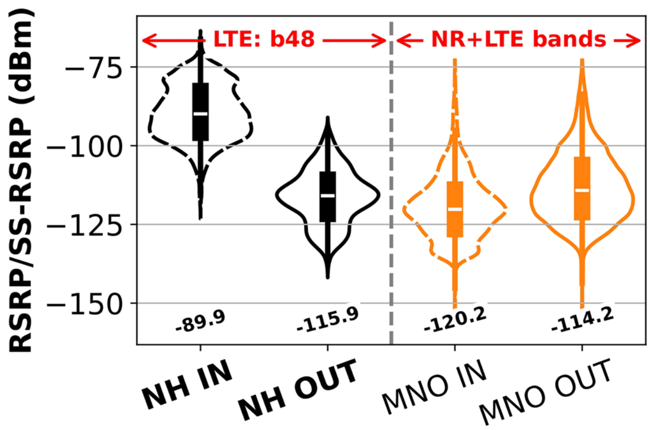

Fig. 5 | RSRP/SS-RSRP comparison over all sites.

Cellular PHY-layer performance comparison

Figure 8 presents the normalized PHY-layer throughput performance across all operators and sites. This metric represents spectral efficiency, thus enabling a fair comparison across heterogeneous deployments[22], i.e.,

$$T_{\text{norm}} = \frac{T_{\text{bps}}}{N_{\text{RB}} \cdot SCS_{\text{Hz}} \cdot 12 \cdot N_{\text{layer}}}, \quad (1)$$

where T_{bps} is the measured throughput in bits/second, N_{RB} is the average number of RBs allocated to the UE per subframe(LTE)/slot(NR), SCS_{Hz} is the subcarrier spacing in Hz, and N_{layer} is the number of MIMO layers used. The term $N_{\text{RB}} \cdot SCS_{\text{Hz}} \cdot 12$ represents the utilized bandwidth, accounting for the 12 subcarriers configured per RB. The results aggregate performance across both low- and mid-band spectrum and are calculated on a per-carrier basis. In Fig. 8, MNO macro performance for both LTE and NR is presented alongside the neutral-host results for a comparative analysis. Because an outdoor small-cell deployment was observed only at Site-A for MNO-A, it was excluded from the comparative PHY and application-level analyses to preserve a uniform macro architecture comparison and avoid operator-specific densification effects.

In the downlink, Fig. 8 indicates no statistically significant difference between indoor neutral-host performance and indoor MNO NR or outdoor MNO LTE macro deployments. In effect, the neutral-host system delivers downlink PHY-layer performance comparable to that of an outdoor LTE macro network. Similar observations have been reported at a different measurement site, as documented in ref. 18. The uplink advantage is evident in Fig. 8, where the NH network delivers substantially higher normalized throughput indoors compared to MNO macro deployments.

A focused indoor mid-band comparison between the neutral-host deployment and MNO macro deployments is presented in Table 7, given that NH b48 operates exclusively in the mid-band spectrum. We observe that the downlink normalized throughput of the neutral-host is 2.48× higher at Site-A, comparable at Site-B, and 0.56× lower at Site-C relative to the MNO mid-band macro. These site-specific variations in downlink performance are consistent with the trends previously observed in Fig. 8, which shows that when aggregated across sites and bands, neutral-host downlink performance remains closely comparable to MNO macro deployments. In contrast, the uplink superiority of neutral-host—already demonstrated in Fig. 8—is further substantiated in Table 7, where the normalized uplink throughput is 2.22× and 6.83× that of MNO mid-band at Sites B and C, respectively. At Site-A, where no measurable uplink performance was observed on MNO mid-band carriers, the neutral-host achieves 1.6 bit/s/Hz/stream. From a resource-normalized performance perspective, the results in Fig. 8 and Table 7 indicate that while neutral-host delivers comparable downlink spectral efficiency to MNO macro deployments, it consistently demonstrates superior uplink efficiency.

Comparison of uplink metrics. The uplink advantage of neutral-host is further supported by the modulation statistics in Fig. 9, which demonstrate a predominant use of higher-order uplink modulation for the neutral-host across Sites A, B, and C. Notably, 64-QAM was employed for approximately 56% of the NH uplink transmission time. Conversely, indoor MNO macro rarely utilizes high-order modulations, with 64-QAM usage limited to about 3% for NR and 6% for LTE.

This is further analyzed through the MCS index measurements shown in Fig. 10. Interestingly, we do not observe a substantial PDSCH MCS index shift between outdoor and indoor environments, despite the measurable building penetration loss discussed earlier. While such attenuation typically affects the Channel Quality Indicator (CQI) reported by the UE, which in turn dictates the PDSCH MCS [22], the downlink remains relatively resilient at these sites. However, a pronounced reduction in the MCS index is consistently observed when transitioning from PDSCH to PUSCH. This finding reinforces that downlink and uplink link quality are inherently asymmetric; while the downlink is buffered by high base station transmit power, the uplink is disproportionately impacted indoors. This suggests that uplink constraints—primarily UE transmit power limitations—play a more dominant role than downlink signal strength alone in limiting higher-order modulation activation.

A further advantage of the neutral-host deployment is the significant reduction in UE power consumption, as illustrated in Fig. 11. The NH UE utilized a median TX power of 18.3 dBm for uplink transmissions—approximately 5 dB lower than the median power required for MNO macro deployments. This improved power efficiency is primarily driven by the proximity of the UE to the indoor CBSDs, which minimizes path loss and allows the UE to maintain a robust link without reaching maximum transmit levels.

Figure 12 summarizes uplink test outcomes across all sites for neutral-host, MNO NR and LTE deployments. Results are based on QualiPoc active probe measurement tests consisting of HTTP upload to *httpbin.org*. A test is classified as failed when the UE is unable to successfully establish a TCP connection with the target server. The analysis reveals that while outdoor MNO macro links experience relatively few failures, the failure rate increases indoors to approximately 28% for NR and 25% for LTE. In contrast, the neutral-host deployment achieves a markedly lower failure rate of about 7%, closely matching the reliability observed for outdoor MNO macro scenarios.

Table 6 | Comparative RSRP/SS-RSRP statistics for MNO & NH networks

Site	Band[a]	IN/OUT	RSRP/SS-RSRP (dBm)		
			Median	P25/P75	Δ[b]
MNO					
Site-A	low-band	IN	−121.4	−126.2/−116.5	9.9
		OUT	−111.5	−117.1/−106.2	
	mid-band	IN	−132.2	−134.6/−125.6	10.7
		OUT	−121.5	−125.9/−116.9	
Small-cell (Site-A)	low-band	IN	−86.9	−90.4/−82.6	9.1
		OUT	−77.8	−84.8/−74.0	
	mid-band	IN	−93.9	−97.7/−90.1	9.9
		OUT	−84.0	−90.9/−76.3	
Site-B	low-band	IN	−112.4	−115.8/−108.5	15.5
		OUT	−96.9	−100.7/−86.7	
	mid-band	IN	−117.6	−122.6/−111.1	17.9
		OUT	−99.7	−108.3/−91.9	
Site-C	low-band	IN	−112.4	−117.1/−105.3	11.1
		OUT	−101.3	−104.2/−99.1	
	mid-band	IN	−116.8	−121.9/−111.2	9.2
		OUT	−107.6	−110.8/−103.6	
Neutral-host					
Site-A	b48	IN	−88.5	−93.7/−80.7	–
Site-B			−89.5	−98.3/−82.8	–
Site-C			−94.3	−99.2/−87.5	–

[a]Low-band refers to frequencies <1 GHz; Mid-band refers to frequencies between 1–7 GHz.
[b]Δ represents building penetration loss.

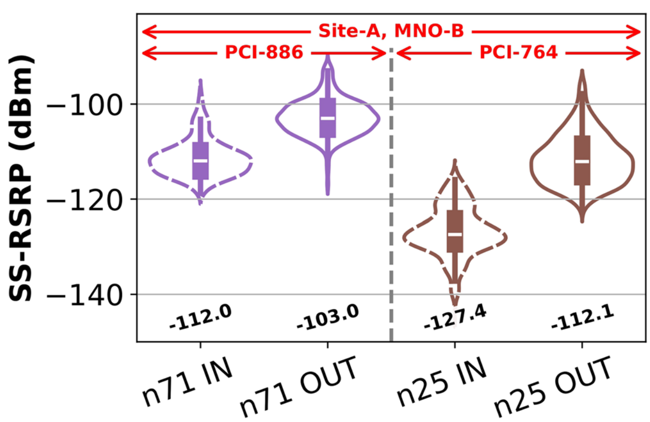

Fig. 6 | Indoor-outdoor RSRP comparison for MNO-B NR low- and mid-band PCIs at Site-A.

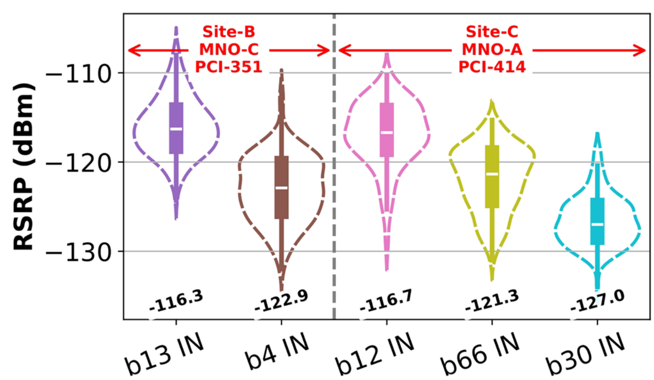

Fig. 7 | RSRP comparison across LTE bands sharing common PCI at Sites B and C.

This highlights the robustness of the neutral-host uplink, particularly in indoor environments where macro coverage is more severely impacted.

Band-specific analysis in the uplink. To further investigate the role of frequency on uplink performance, we examine NR operations across low- and mid-band spectrum. The wider bandwidth of mid-bands (i.e., n41 and n77) enables superior peak rates. However, their indoor uplink remains constrained by the previously discussed propagation and power limitations, hindering their overall efficacy in indoor settings.

Figure 13 illustrates the relative usage of low- and mid-band spectrum across environments. For Sites B and C, a pronounced shift toward mid-band utilization is observed in outdoor scenarios, with mid-band usage increasing from approximately 68% indoors to complete usage outdoors at Site-B, and from about 36% indoors to complete usage outdoors at Site-C. These observations indicate that, even when mid-band NR coverage is available—as evidenced by its dominant usage outdoors—UEs tend to avoid mid-band operation indoors. This behavior underscores the importance of low-band spectrum for indoor uplink, likely due to its superior propagation and penetration characteristics. At Site-A, no NR band usage is observed indoors, suggesting a comparatively weak NR deployment by the MNOs. Outdoors, NR operation at this site is dominated by low-band usage, indicating that, under limited deployment conditions, UEs preferentially select low-band spectrum to maintain reliable uplink connectivity.

Comparison of end-to-end network performance

To evaluate end-user performance and facilitate a direct comparison with Wi-Fi, we utilized application-based metrics from HTTP and ICMP traffic. Specifically, the metrics are measured at the network/IP layer, with DL and UL throughput measured using HTTP GET and POST traffic, respectively,

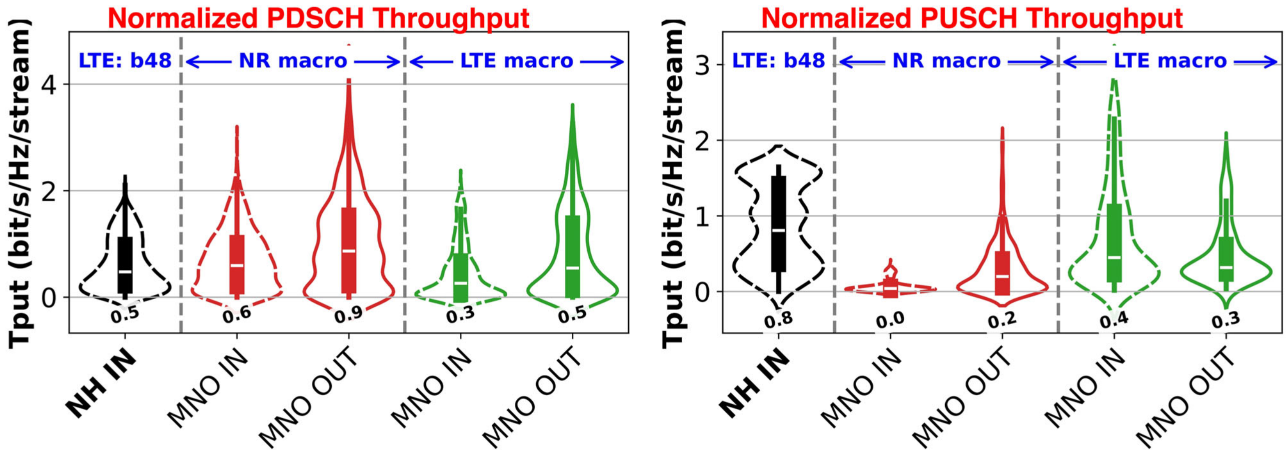

Fig. 8 | Normalized throughput comparison over all sites.

Table 7 | Site-wise normalized throughput comparison between NH b48 and mid-band MNOs

Site	Location	Network	DL Tput[a]	UL Tput[a]
Site-A	Indoor	NH b48	1.12	1.60
		MNO mid-band	0.45	–
Site-B	Indoor	NH b48	0.55	0.98
		MNO mid-band	0.64	0.44
Site-C	Indoor	NH b48	0.32	0.41
		MNO mid-band	0.57	0.06

[a]Median of LTE+NR normalized PDSCH/PUSCH throughput.

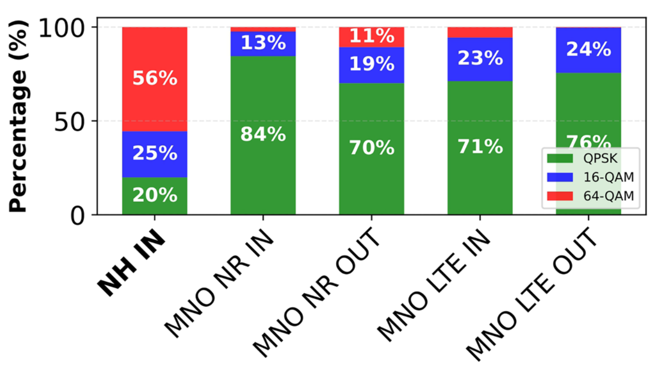

Fig. 9 | Uplink modulation usage distribution.

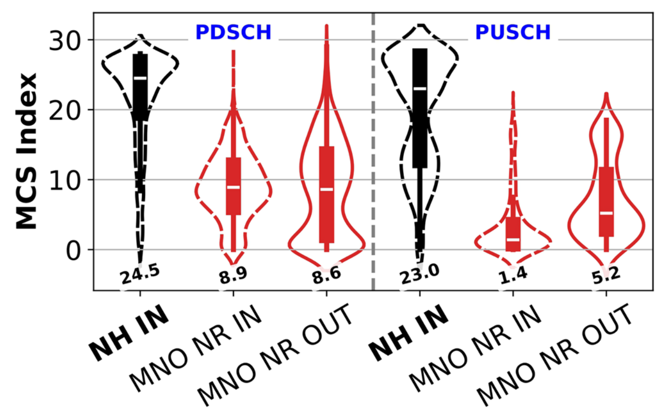

Fig. 10 | PDSCH and PUSCH MCS index distributions.

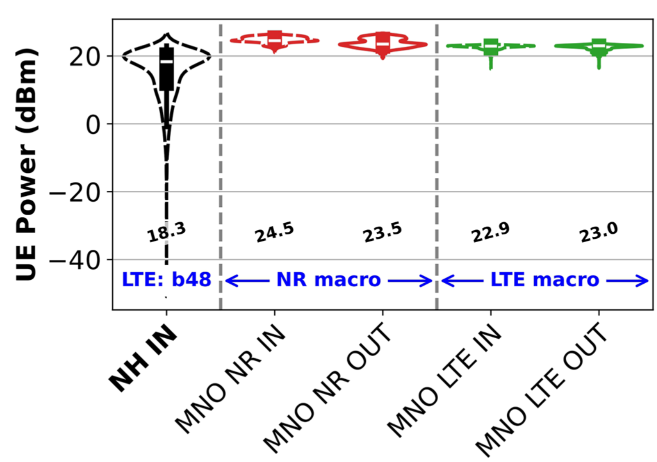

Fig. 11 | Uplink TX power.

while the round-trip time is measured via ICMP echo requests. Unlike PHY-layer metrics, which characterize raw radio capacity, these measurements capture end-to-end performance as observed by user traffic, including protocol overheads, scheduling effects, and network-side processing.

Figure 14 summarizes the distributions of indoor DL and UL throughput and round-trip time for NH, MNO macro, and enterprise Wi-Fi networks across all sites. The results indicate that NH median DL and UL throughput slightly surpass MNO macro levels, highlighting the efficacy of the NH model in overcoming indoor penetration loss. Nevertheless, Wi-Fi maintains a significant lead in UL throughput. On latency, there is a clear hierarchy with NH exhibiting the longest RTT, followed by MNO and Wi-Fi. This latency penalty in NH networks is primarily attributed to the additional routing overhead incurred during packet delivery to the MNO core.

To further examine performance differences, a per-site breakdown between NH and Wi-Fi is provided in Table 8. This comparison is particularly robust as both networks utilized identical backhaul infrastructure at each site and operated with comparable channel bandwidths.

At Site-A, where NH operates at 40 MHz and Wi-Fi at 20 MHz for downlink, the neutral-host achieves an approximately 2.3× higher median DL throughput. At Sites B and C, both technologies operate with comparable 40 MHz downlink bandwidth, with NH achieving a slightly lower median DL throughput (0.7× at Site-B and 0.9× at Site-C). These trends underscore the primary influence of spectral allocation on downlink performance and demonstrate that NH can match enterprise Wi-Fi capacity with a significantly smaller hardware footprint, as evidenced by the lower CBSD count.

In the uplink, the trends diverge. At Site-A, both neutral-host and Wi-Fi operate with matching 20 MHz uplink bandwidth, yet Wi-Fi achieves an approximately 1.8 × higher median UL throughput. This gap is further amplified in Sites B and C, where NH operates at 20 MHz while Wi-Fi at 40 MHz. In these sites, Wi-Fi median UL throughput exceeds that of NH by factors of 10.7× and 4.5×, respectively. A similar pattern is observed for round-trip time, where Wi-Fi consistently achieves lower latency across all sites.

Several factors likely contribute to the suboptimal UL throughput and latency performances observed in the NH network. These include fundamental protocol differences: the 4G-based NH operates under a TDD configuration that restricts uplink transmission to specific subframes, whereas Wi-Fi utilizes a contention-based mechanism. Additionally, neutral-host traffic must be routed to the respective MNO core network, whereas Wi-Fi traffic follows a more direct local path. Additionally, it is important to note that the specific choice of NH network architecture intrinsically impacts the observed latency performance. The gateway-based architecture in our testbed introduces unavoidable overhead, including additional network hops, Network Address Translation (NAT) processing, and IPsec tunneling encapsulation. This architecture runs opposite to the traditional MOCN architecture, which requires dedicated lines (e.g., fiber, carrier-grade Ethernet) for the MNO cores to be integrated into the shared RAN. Thus, the gateway model trades the latency performance for a massive increase in deployment flexibility and cost-effectiveness.

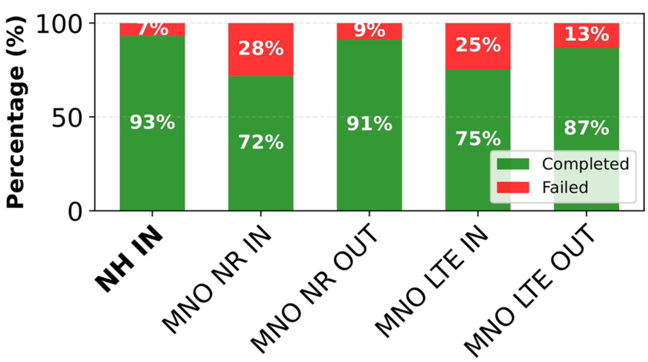

Fig. 12 | Uplink HTTP upload test status statistics.

Discussion

Our analysis of NH, MNO macro, and Wi-Fi deployments at their sites with distinct signal environments shows:

- There is a significant indoor coverage gap for MNO macro networks, with building penetration losses reaching 15.5 dB in the low bands 17.9 dB in the mid-bands. With median mid-band signal RSRP trailing low-bands by roughly 10 dB in both indoor and outdoor environments, it is evident that low-band frequencies serve as the primary choice for indoor connectivity.
- Small-cell analysis at Site-A confirms that proximity drastically improves indoor coverage, with median RSRP gains of 34.5 dB and 38.1 dB for low- and mid-bands, respectively. Despite these gains, mid-band RSRP continues to trail low-band by up to 7 dB, mirroring the

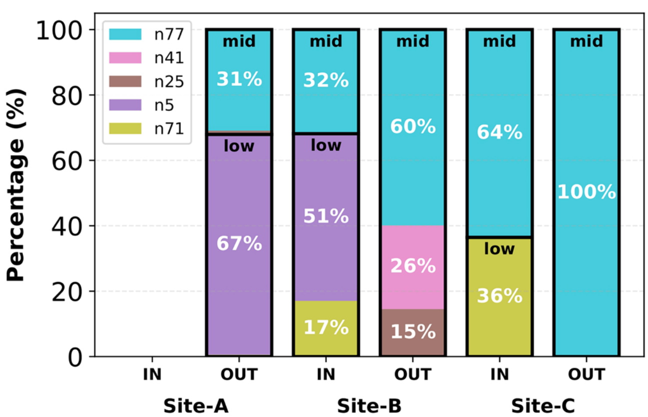

Fig. 13 | NR uplink band usage distribution across indoor and outdoor.

Table 8 | Site-wise indoor application-layer (IP) performance summary

Site	Network	#PCIs[a]/#BSSIDs[b]	DL Tput[c]	UL Tput[c]	RTT[c]
Site-A	NH	10	79.72	24.15	120
	Wi-Fi	67	34.9	44.02	46
Site-B	NH	6	32.02	15.01	90
	Wi-Fi	244	44.54	161.02	28
Site-C	NH	8	17.75	5.44	74
	Wi-Fi	230	19.46	24.56	25

[a]Each CBSD is configured with two PCIs.
[b]2.4, 5 GHz counted separately.
[c]Median value.

Fig. 14 | Comparison of network layer throughput and RTT.

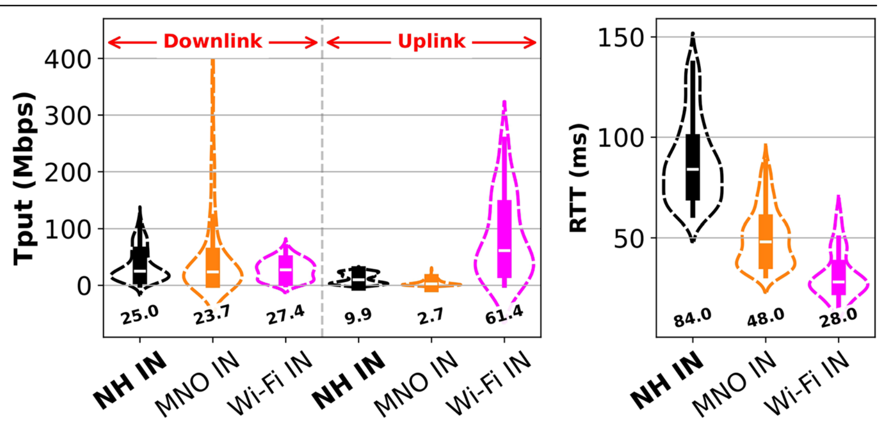

frequency-dependent propagation characteristics observed in macro deployments.
- Per-PCI analysis further confirms the frequency-dependent nature of indoor attenuation by isolating signals from a single base-station source. Across both NR and LTE deployments, higher-frequency bands consistently exhibit larger indoor signal degradation than lower-frequency bands.
- Due to a 30.3 dB improvement in median indoor RSRP over MNO macro-cells, the NH network delivers normalized indoor downlink throughput that exceeds indoor MNO benchmarks and matches MNO outdoor performance. The advantage is even more pronounced in the uplink, where the indoor NH solution surpasses MNO performance regardless of the MNO UE's environment (indoor or outdoor).
- NH networks utilize 64-QAM modulation for 56% of indoor uplink transmissions, whereas MNO macro networks achieve this only 3% (NR) and 6% (LTE) of the time. Furthermore, NH UEs benefit from a 5 dB reduction in median transmit (TX) power. These performance gains are directly enabled by the proximity of UEs to the indoor CBSDs, which minimizes path loss and ensures a robust link budget.
- NH networks also maintain higher PHY-layer MCS indices overall, while macro deployments show a marked reduction from downlink to uplink MCS, highlighting the intrinsic downlink–uplink asymmetry and reinforcing that UE transmit power limitations are a primary constraint on indoor uplink performance.
- While mid-bands are utilized extensively for outdoor 5G traffic, MNOs revert to low-band spectrum for the indoor uplink. This shift underscores the propagation constraints of mid-band frequencies, which often fail to maintain a reliable indoor uplink link budget due to high building attenuation.
- The neutral-host network outperforms MNOs in indoor end-to-end throughput, but trails Wi-Fi in UL throughput and latency. Specifically, Wi-Fi surpasses NH in median uplink throughput by up to 1.8× under matched 20 MHz bandwidth, and by up to 10.7× when utilizing 2× the NH bandwidth. These results underscore the necessity of protocol and routing optimizations to achieve full parity in uplink and latency-sensitive performance.

Looking ahead, a key area for further investigation is a deeper, controlled comparison between Wi-Fi and neutral-host systems. The results presented here are derived from customer-facing infrastructure, where deployment parameters cannot be systematically controlled to enable rigorous, apples-to-apples evaluation. To address this limitation, the University of Notre Dame has recently deployed a co-located experimental testbed comprising Wi-Fi 6E (operating in the unlicensed 6 GHz band) and neutral-host infrastructure (operating in the CBRS 3.5 GHz shared band). This testbed will enable targeted studies of several open research questions, including (i) the impact of neutral-host handover mechanisms—from MNO networks and across CBSDs—relative to inter-AP Wi-Fi handovers, and (ii) uplink throughput and latency behavior, which remain critical yet comparatively underexplored dimensions in Wi-Fi versus neutral-host performance evaluations.

Data availability

The data supporting the findings of this study are available under license from Celona, Inc. and are not publicly available due to proprietary restrictions. However, anonymized datasets (stripped of specific operator and geospatial identifiers) are available from the corresponding author upon reasonable request and with the express permission of Celona, Inc.

Received: 8 January 2026; Accepted: 12 April 2026;
Published online: 04 August 2026

References

1. *5G Observatory Report 2025*. https://digital-strategy.ec.europa.eu/en/policies/5g-observatory-2025 (European Commission, 2025).
2. Ericsson Consumer & Market Insight. *Five Ways to a Better 5G: Key Trends Influencing Consumer Adoption of 5G*. https://www.ericsson.com/en/reports-and-papers/consumerlab (2021).
3. ChosunBiz. *Government cuts LTE reassignment fee to 3.1 trillion won, ties further discounts to 5G indoor base station buildout*. https://biz.chosun.com/en/en-it/2025/12/10/CPEBGUFQBVA27ICHZMH3TT4T2Q/ (2025).
4. Ericsson. *Ericsson Mobility Report: June 2025*. https://www.ericsson.com/en/reports-and-papers/mobility-report (2025).
5. Sathya, V., Shah, M. & Yavuz, M. Neutral host deployment-a measurement study on routing and mobility management between public and private network. In *Proc. 2023 IEEE Future Networks World Forum (FNWF)* 1–8, https://doi.org/10.1109/FNWF58287.2023.10520510 (2023).
6. 3rd Generation Partnership Project. Universal Mobile Telecommunications System (UMTS); LTE; Network sharing; Architecture and functional description (3GPP TS 23.251 version 14.0.0 Release 14). https://www.etsi.org/deliver/etsi_ts/123200_123299/123251/14.00.00_60/ts_123251v140000p.pdf (2017).
7. National Telecommunications and Information Administration. The National Spectrum Strategy. https://www.ntia.gov/sites/default/files/publications/national_spectrum_strategy_final.pdf (2023).
8. The White House. Winning the 6G race. Presidential Memorandum. https://www.whitehouse.gov/presidential-actions/2025/12/national-security-presidential-memorandum-nspm-8-0bda/ (2025).
9. Ghosh, M. The upper C-Band notice of proposed rulemaking. *IEEE Wirel. Commun.* **33**, 11–12 (2026).
10. Ghosh, M., Shuvo, S. M. H. A., Palathinkal, J. R. & Rochman, M. I. Reply comments on FCC's NPRM on the upper C-band, Docket 25-59. https://www.fcc.gov/ecfs/document/1021988035423/1 (2026).
11. Ghosh, M., Palathinkal, J. R., Rochman, M. I. & Shuvo, S. M. H. A. Filing detail; reply comments on FCC's NPRM on the upper C-band, Docket 25-59. https://www.fcc.gov/ecfs/search/search-filings/filing/10121176025934 (2026).
12. Bajracharya, R., Shrestha, R., Jung, H. & Shin, H. Neutral host technology: the future of mobile network operators. *IEEE Access* **10**, 99221–99234 (2022).
13. Allawi, Y. M. et al. Cost-efficient citywide neutral host design: a micro-operator business model for expedited 5G and beyond network infrastructure rollout. *IEICE Trans. Commun.* **E108-B**, 450–464 (2024).
14. Fernández-Fernández, A. et al. Validating a 5G-enabled neutral host framework in city-wide deployments. *Sensors* **21**, 8103 (2021).
15. Arendt, C., Fricke, S., Böcker, S. & Wietfeld, C. Distributed performance evaluation of 5G and Wi-Fi for private industrial networks. In *Proc*. *2024 IEEE 35th International Symposium on Personal, Indoor and Mobile Radio Communications (PIMRC)* 1–7 (IEEE, 2024).
16. Arendt, C., Böcker, S., Bektas, C. & Wietfeld, C. Better safe than sorry: distributed testbed for performance evaluation of private networks. In *Proc. 2022 IEEE Future Networks World Forum (FNWF)* 190–196 (IEEE, 2022).
17. Rochman, M. I., Roy Palathinkal, J., Sathya, V., Yavuz, M. & Ghosh, M. Neutral-hosts in the shared mid-bands: addressing indoor cellular performance. In *Proc. 2025 IEEE International Symposium on Dynamic Spectrum Access Networks (DySPAN)*, 1–9 (2025).
18. Palathinkal, J. R., Rochman, M. I., Sathya, V., Yavuz, M. & Ghosh, M. Indoor sharing in the mid-band: a performance study of neutral-host, cellular macro, and wi-fi. In *2026 IEEE 23rd Consumer Communications & Networking Conference (CCNC),* 1–6) (IEEE, 2025).
19. Tusha, A. et al. A comprehensive analysis of secondary coexistence in a real-world CBRS deployment. *IEEE Transactions on Cognitive Communications and Networking* (2025).

20. Rohde & Schwarz. QualiPoc Android. https://www.rohde-schwarz.com/us/products/test-and-measurement/network-data-collection/qualipoc-android_63493-55430.html (2025).
21. Doğan-Tusha, S., Tusha, A., Rochman, M. I., Nasiri, H. & Ghosh, M. Spectrum sharing characterization using smartphones: exploring 6 GHz sharing through large-scale wi-fi 6E measurements. *IEEE Commun. Mag.* **63**, 70–76 (2025).
22. Rochman, M. I., Ye, W., Zhang, Z.-L. & Ghosh, M. A Comprehensive real-world evaluation of 5G improvements over 4G in low-and mid-bands. *IEEE Transactions on Cognitive Communications and Networking* (2025).

Acknowledgements
Works in this paper by authors J.R.P., M.I.R., and M.G. are supported by the National Science Foundation (NSF) grant numbers CNS-2229387 and AST-2132700.

Author contributions
The contributions are as follows: J.R.P. wrote the main manuscript text, performed the primary data analysis, and prepared all figures except for Fig. 2. M.I.R. contributed to the formal analysis and provided major text refinements and critical revisions. V.S. curated the source data and prepared Fig. 2. M.G. and M.Y. provided overall project supervision and secured the necessary resources. All authors reviewed and approved the final manuscript.

Competing interests
The authors declare no competing interests.

Additional information
Correspondence and requests for materials should be addressed to Joshua Roy Palathinkal.